Computational Materials Science 84 (2014) 350–354

Contents lists available at ScienceDirect

Computational Materials Science

journal homepage: www.elsevier.com/locate/commatsci

First-principles study of the structural, electronic and optical properties of tetragonal $LiIO_3$

Gang Yao [a,b], Xinyou An [c], Yu Chen [d], Yajun Fu [a], Zhongqian Jiang [a], Yiding Liu [b,*]

[a] School of Materials Science and Engineering, Southwest University of Science and Technology, Mianyang 621010, PR China
[b] College of Physics and Electronic Engineering, Leshan Normal University, Leshan 614004, PR China
[c] Department of Physics and Electronic Information, China West Normal University, Nanchong 637002, PR China
[d] College of Science, Inner Mongolia University of Technology, Hohhot 010051, PR China

ARTICLE INFO

Article history:
Received 1 May 2013
Accepted 12 December 2013
Available online 9 January 2014

Keywords:
Density-functional theory
Electronic structure
Optical properties
Tetragonal $LiIO_3$

ABSTRACT

The structural parameters, electronic structure, chemical bonding, and optical properties of tetragonal $LiIO_3$ have been studied using the *ab initio* pseudopotential density functional method within the generalized gradient approximation. The structural parameters of tetragonal $LiIO_3$ agree well with the experimental data. Results are given for bulk modulus B and its pressure derivative B_0'. The energy band structure, density of states, and Mulliken charge population are obtained, which indicates that tetragonal $LiIO_3$ has an indirect band gap of 2.65 eV at A–Γ, in the absence of the scissors operation. Furthermore, in order to clarify the mechanism of optical transitions of tetragonal $LiIO_3$, the complex dielectric function $\varepsilon(\omega)$, refractive index $n(\omega)$, extinction coefficient $\kappa(\omega)$, absorption efficient $\alpha(\omega)$, reflectivity $R(\omega)$ and energy loss function $L(\omega)$ are also calculated.

1. Introduction

Lithium iodate ($LiIO_3$) crystal attracts attention mainly due to the diversity in its crystal structure such as: α-type, C_6^6 ($P6_3$) [1], β-type, C_{4h}^4 ($P4_2/n$) [2], ξ-type, ($P2_12_12_1$) [3,4], γ-type, ($Pna2_1$) [5], and other intermediate phases such as C_{2h}^4 ($P2/n$) [6], ($P121/n1$), and C_{2h}^4 ($P2/n$) [4]. Among the numerous phases of $LiIO_3$, α-type, C_6^6 ($P6_3$) has been used widely in optoelectronic applications due to its elasto-optic [7], electro-optical properties [8], large transparency range [8], strong piezoelectric [9] and high non-linear coefficients [10–12]. People have carried on a large amount of research on the experiment and theory, and make $LiIO_3$ gain enormous development. There are only a few studies, however, on the photorefractive effect in pure and impurity-doped crystals [13,14], which also has attracted more attention [15–17].

Unlike the α-phase, β-$LiIO_3$, (C_{4h}^4 ($P4_2/n$), tetragonal structure) does not possess any piezoelectric or nonlinear-optical properties [6]. Previous investigations have been devoted to study the physical properties and structural changes of the $LiIO_3$ crystal [4–6, 18–21]. In 1970, Becker et al. [21] reported upon cooling from 300 to 7 K, the absorption coefficients of $LiIO_3$ decrease drastically in the 10–150 cm^{-1} spectral region. This characteristic is important for far-infrared generation by mixing of two laser frequencies. The pressure-induced phase transition in β-$LiIO_3$ was first observed by Lemos et al. [5] with pressure Raman experiment in 1983 and analysis of their results showed that the crystal undergoes an abrupt reversible structural phase transition to a new (δ-$LiIO_3$) at about 50 kbar hydrostatic pressure. Afterwards, Mendes Fílho et al. [6] conducted more detailed studies to characterize structural aspects of the β-$LiIO_3$ phase transition by means of high-pressure X-ray diffraction, and the compressibility of the material in its two phases was also been measured. In 1989, the polymorphism phase transition and relative stability of various phases in $LiIO_3$ crystal at normal pressure have been further studied by Liang et al. [4] with *u*DTA, constant-temperature heat treatment, specific heat, and room- and high-temperature powder X-ray diffractions technique.

At present, however, there are no reports about the electronic and optical properties of tetragonal $LiIO_3$. We therefore think that it is worthwhile to perform calculations for the structural, electronic, and optical properties of tetragonal $LiIO_3$ material using the first-principles calculations, which can provides insight into the nature of the solid-states theories and determines the values of fundamental parameters [22]. The paper is organized as follows: in the next section, we will give the technical details of our employed methods. Section 3 is devoted to the results and discussion, including geometry and structural properties, electronic and chemical bonding, and optical properties. Finally, our main findings are given in Section 4. And many useful results have been obtained, which offers theoretical data for the design and application for tetragonal $LiIO_3$ in photoelectric materials.

* Corresponding author. Tel.: +86 13438473603.
E-mail address: newonenail@sina.com (Y. Liu).

0927-0256/$ - see front matter © 2014 Elsevier B.V. All rights reserved.
http://dx.doi.org/10.1016/j.commatsci.2013.12.025

2. Computational methodology

Our calculations are performed with the Cambridge Serial Total Energy Package (CASTEP) code [23], based on density-functional theory (DFT) and plane-wave pseudopotential technique. Generalized gradient approximation (GGA) with the Perdewe Wang 1991 (PW91) exchange-correlation functional [24] was used. The ion–electron interaction was modeled by ultrasoft pseudopotentials [25]. The valence-electron configurations for the elements of tetragonal $LiIO_3$ discussed in this paper are O $2s^2 2p^4$, Li $2s^1$, and I $5s^2 5p^5$. We choose the energy cutoff to be 600 eV, and the numerical integration of the Brillouin zone (BZ) was performed using $5 \times 5 \times 6$ Monkhorst-Pack (MP) [26] k-point sampling. Structure parameters were fully relaxed using the BFGS minimization method [27], in which free movement of the atoms in any direction is allowed and no symmetry constraint is imposed. Careful convergence tests show that with these parameters relative energy converged to better than 5×10^{-7} eV/atom.

3. Results and discussion

3.1. Geometry and structure optimization

We used the X-ray diffraction data [28] as a starting point for geometry optimization. The lattice parameters ($a = b$, c in Å), bulk modulus B and its pressure derivative $B_0' = (dB/dp)_{p=0}$ were calculated and fitted to third order Birch-Murnaghan equation of states [29] (see Fig. 1). The calculated results compared with available experimental data for tetragonal $LiIO_3$ are summarized in Table 1.

The computed lattice parameters a and c are 9.723 and 6.269 Å, respectively, which approximately consist with the intrinsic ones [30,31]. More importantly, the calculated mass density for tetragonal $LiIO_3$ is 4075.98 Kg/m^3, in close agreement with experimental value 4091.28 Kg/m^3 [31]. Such agreement demonstrates that the computational methodology used in this work is suitable and the results from our geometry optimizations are reliable. Additionally, the differences from experimental results could be due to the use of an approximate DFT and the GGA leads to overestimate data in relation to the experimental data. Moreover, the bulk modulus B (67.402 GPa) and its pressure derivative B_0' (4.619) were calculated for the first time, which remains to be proven in trials.

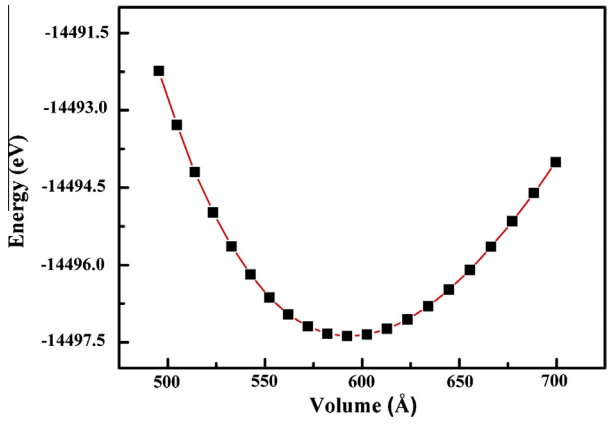

Fig. 1. Total energy as a function of volume for tetragonal $LiIO_3$.

Table 1
Calculated and experimental lattice parameters, bulk modulus B, and its pressure derivative B_0' of tetragonal $LiIO_3$.

	a (Å)	c (Å)	V (Å^3)	Mass density (Kg/m^3)	B (GPa)	B_0'
This work	9.723	6.269	592.651	4075.98	67.402	4.619
Expt. [28]	9.66	6.21	579.49	4208.33	–	–
Expt. [30]	9.733	6.157	583.21	4141.96	–	–
Expt. [31]	9.7899	6.1605	590.44	4091.28	–	–

3.2. Electronic and chemical bonding

The energy band structure of tetragonal $LiIO_3$ along with the high-symmetry points of the Brillouin zone is shown in Fig. 2. The energy scale is in eV and the top of the valence band was set to zero in the energy scale. An indirect band gap of 2.65 eV (without empitical correction factor) is seen in the direction (A–Γ) between the top of the valence band at point A and the bottom of the conduction band at point Γ. The top of the valence band (VB) and the bottom of the conduction band (CB) are composed of O $2p$ states and I $5p$ states. Table 2 presents band gap energies along with the valence-to-conduction band transition for tetragonal $LiIO_3$, which are the important features of the band structure for this compound. As we all know, the DFT calculations usually underestimate the band gap of semiconductors [32–34]. So the true gap of tetragonal $LiIO_3$ should be larger than the computed gap of 2.65 eV. In our calculation, the scissor operators on both the electronic structure and the optical properties were not considered.

By analyzing the partial density of states (PDOS) (see Fig. 3), it was found that the O $2p$ states have some admixture with the I $5p$ states, *i.e.* $LiIO_3$ appears to have some covalent features. The energy bands at about −43 eV consist of Li $2s$ states showed a sharp peak due to its strong localization character. The conduction bands are mostly composed of O $2p$ and I $5p$ states. Taken together, the energy state density curve near the Fermi level mainly come

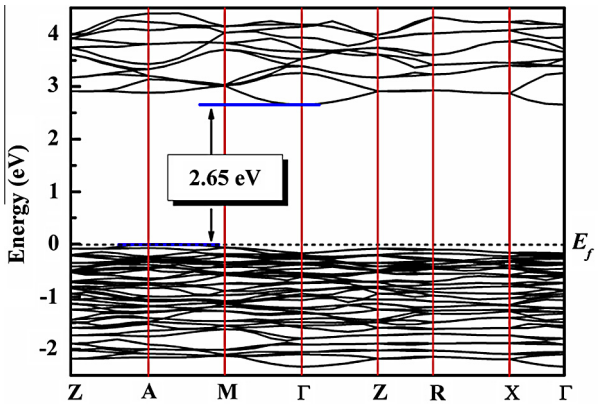

Fig. 2. Band structure of tetragonal $LiIO_3$ along the high-symmetry points of the Brillouin zone at the equilibrium lattice constant. The energy zero is taken at E_f.

Table 2
Band gap energies E_g and symmetry of the valence to conduction band transition for tetragonal $LiIO_3$.

Valence to conduction band transition	Band gap energies (eV)
$A \rightarrow \Gamma$	2.652
$Z \rightarrow Z$	2.995
$A \rightarrow A$	2.892
$M \rightarrow M$	3.086
$\Gamma \rightarrow \Gamma$	2.821
$R \rightarrow R$	3.036
$X \rightarrow X$	3.040